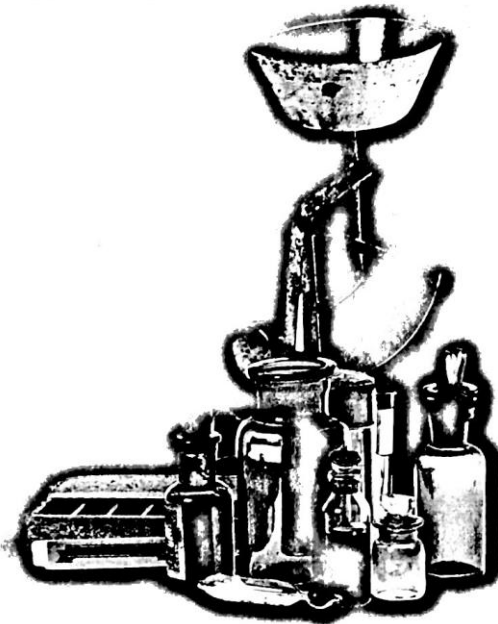


# CHEMTECH '14

## CHEMICAL ENGINEERING AND CHEMICAL TECHNOLOGIES CONFERENCE



CONTENTS

9	CHEMICAL ENGINEERING & CHEMICAL TECHNOLOGIES	
11	IN-PERSON PRESENTATIONS	
13	SIMULATION OF THE POWER CABLE PROCESSING VANJA KOSAR	
23	LOW LEVEL LIQUID HANDLING IN CRUDE DISTILLATION COLUMN TRAYS ANSHUL ARORA, VIJAY SINGH R.	
35	THIN LAYER DRYING MATHEMATICAL MODELLING OF ORTHOSIPHON STAMINEUS HERBAL PLANT LEAVES USING PAGE MODEL SRIYAMA ABDULLAH, ABDUL RAZAK SHAARI, IBHI HAJAR RUKUNUDIN, MUHAMMAD SYARHABIL AHMAD	
47	AUGMENTATION OF HEAT TRANSFER AND TURBULENCE FOR BETTER PERFORMANCE OF PHOTOVOLTAIC PANEL SYED MOHD YAHYA, SYED FAHAD ANWER AND SAMEEY SANGHI	
57	FT-IR STUDY OF THE NANOSURFACE PHENOMENA OF METALLIC NANOPARTICLES AND NANOWIRES I. MARKOVA - DENEVA	
73	SUBCLONING AND EXPRESSION OF RECOMBINANT HUMAN PARATHYROID HORMONE RHPTH BY FUSION STRATEGY IN E.COLI SADEGH MAJDI, ELAHE ESFAHANI, HOSSEIN AMANI, GHASEM NAJAF POUR D, MAJID SHAHBAZI	
85	SYNTHESIS OF THE FATTY ACID METHYL ESTER CATALYZED BY IONIC LIQUIDS WOJCIECH KRASODOMSKI AND JOANNA OLEKSIK	
87	SYNTHESIS OF THE FATTY ACID METHYL ESTER CATALYZED BY CATIONITES JOANNA OLEKSIK AND WOJCIECH KRASODOMSKI	
89	ZEOLITE SYNTHESIS FROM TUNGBILEK FLY ASH WITH ALKALINE HYDROTHERMAL METHOD: EFFECT OF NAOH/FLY ASH RATIO ÖZGÜL DERE ÖZDEMİR AND SABRIYE PİSKİN	
97	CHARACTERIZATION OF THE BERGAMA GOLD MINE WASTE F. DUR, M. YILDIRIM, A. S. KIPÇAK, E. MOROYDOR DERUN, S. PİSKİN	
105	ULTRASONIC SYNTHESIS OF COPPER BORATES AT 70°C S. KAVCI, F. T. SENBERBER, A. S. KIPÇAK, E. MOROYDOR DERUN, S. PİSKİN	
111	THE INVESTIGATION OF THE ELEMENT CONTENTS IN THE APPLE JUICE F. DEMİR, A. S. KIPÇAK, Ö. DERE ÖZDEMİR, E. MOROYDOR DERUN, S. PİSKİN	
121	THE INVESTIGATION OF THE ELEMENT CONTENTS IN THE CLASSIC, DECAF AND FILTER COFFEES A. S. KIPÇAK, F. DEMİR, Ö. DERE ÖZDEMİR, E. MOROYDOR DERUN, S. PİSKİN	
131	DETERMINATION OF THE ZINC SULFATE, TINCALCONITE AND BORIC ACID MOLAR RATIO IN THE PRODUCTION OF ZINC BORATES A.S. KIPÇAK, F.T. SENBERBER, E. MOROYDOR DERUN, M. TUGRUL, S. PİSKİN	
139	REGIOSELECTIVE REDUCTION OF THE ENONE SYSTEM TO DIENE SYSTEM KHALED SHAWKATEN, RAED AL-ZOUBI	
141	DEVELOPMENT OF METHODOLOGY FOR THE DETERMINATION OF PHENIBUT IN MEDICINES PHD L. LOGOYDA, DR. D. KOROBKO, PHD N. ZARIYVA	
155	NANOSCALE CHARACTERIZATION OF BIMETALLIC Au-Cu SUPPORTED NANOPARTICLES SUMEYA BEDRANE, WAHIBA BENEDEDDOUCHE, ZOLUKHA FANDI, REDOUANE BACHIR	
157	MILD COMMON AGENTS FOR SUPPRESSING P. CANALICULATA EGGS HATCHABILITY NOOR HASYIERAH MOHD SALLEH, DACHYAR ARBAIN, WIRDA AYUNI	
165	THE EFFECTS OF ZNO CRYSTALS ON THE BARRIER PROPERTIES OF LOPE POLYMER TUGCE BEKAT, MUALLA ONER	
167	PRODUCTION AND CHARACTERIZATION OF SILICA AEROGELS FROM RICE HULL ASH SILICA TÜLAY MERVETEMEL, SEVİL YÜCEL, YELİZ ELALMIŞ, BURCU KARAKUZO	
173	FORMULATION OF BIOADHESIVE GELS USING MODIFIED CARRAGEENANS N. MÖDLAI-WÖSTEFÄ, S. LEFNAOUI	
175	POSTER PRESENTATIONS	
177	SYNTHESIS OF DENDRIMERS USED AS SORBENTS, BASED ON THE FORMATION OF COPOLYMER FOR CAPTURE ORGANIC ACIDS RICARDO CASTRO CEPEDA, LUIS GUZMAN JOFRE, OSCAR VALDES, LEONARDO SILVA SANTOS, ADOLFO MARICAN, CLAUDIA VERGARA	
179	ENHANCED CR6+ ADSORPTION CAPACITY OF THE NEW POLY(ACRYLAMIDE)/ MONTMORILLONITE NANOCOMPOSITE HYDROGELS BY IMMOBILIZING SPIRULINA MICROALGAE DEMET AYDINOĞLU, ÖZKAN ANKÜL, VILDAN BAYRAM, SINAN ŞEN	
181	CHEMICAL CHARACTERIZATION OF WASTE WATER OF INDUSTRIAL UNIT IN ANNABA AREA (ALGERIA) MOMAHED KAHOUŁ AND MASSIMA DERBAL	
183	HYDROLYSIS STUDY ON THE ROOM TEMPERATURE IONIC LIQUID/WATER MIXTURE BY 19F AND 11B NMR: N,N-DIETHYL-N-METHYL-N-(2-METHOXYETHYL)AMMONIUM TETRAFLUOROBORATE KOJI SAHARA, HIDEYUKI FUJIMOTO, YUKIHIRO YOSHIMURA, AKIO SHIMIZU,	
185	EFFECT OF PRESSURE AND TEMPERATURE ON THE VIABILITY, MORPHOLOGY AND FUNCTION OF RAT PRIMARY ASTROCYTES KEJI NEI, KAZUYUKI NAKAJIMA, SHINICHI YAMAMOTO, AKIO SHIMIZU,	
187	AGGREGATION BEHAVIOR OF SYMMETRICAL AND UNSYMMETRICAL 1,3-DIALKYLIMIDAZOLIUM BROMIDES IN AQUEOUS SOLUTIONS MINORU SAITO, KAZUMA ABE, MASATO ITO AND AKIO SHIMIZU	
189	STUDY OF THE INFLUENCE OF HIGH HYDROSTATIC PRESSURE PROCESSING ON PRESERVATION AND FREE AMINO ACID OF MINCED FISH AYAKO YAMASAKI AND AKIO SHIMIZU	
191	SYNTHESIS OF 3,4-DIHYDROPRIMIDINONE USING ZINC NITRATE AS A CATALYST UNDER SOLVENT FREE CONDITIONS KAHINA KOUACHI, LEILA BENNINI, SALHA MENAD,	
193	EFFECT OF THE ZEOLITE STRUCTURE ON THE PHOTOCATALYTIC DEGRADATION OF METHYLENE BLUE ON TiO2ZEOLITES GHANIA FOURA AND AHCÈNE SOUALAH	

- 195 ONE-POT SYNTHESIS OF 3,4-DIHYDROPRIMIDIN-2(1H)-ONES: VARIATION OF SOLVENT AND THE AMOUNT OF HCL  
LEILA BINNINI, SALHA MENAD, KAHINA KOUACHI,
- 197 OPTIMIZATION STUDIES FOR TARTARIC ACID RECOVERY FROM INDUSTRIAL RED AND WHITE TARTAR WASTES  
MAHENDRA ARYAL AND MARIA LIKOPOULOU-KYRIAKIDES
- 199 ANTIOXIDANT ACTIVITY OF THE EXTRACTS DERIVED FROM WINE INDUSTRY BYPRODUCTS AND CORRELATION TO THEIR ANTHOCYANIN CONTENT  
EVANGELOS TRIKAS, MARIA MELIDOU, RIGINI PAPI, GEORGE ZACHARIADIS AND DIMITRIOS KYRIAKIDIS
- 201 FLOW PHENOMENA OF DROPLETS IN T-JUNCTION MICROCHANNELS USING MICRO-PIV  
TSUNG-SHENG SHEU, BO-RENG PENG, HERCHANG AY,
- 203 NEW DISCRETE SQUARE METAL-DNA NANOSTRUCTURES: SYNTHESIS, SELF-ASSEMBLY, AND CHARACTERIZATION  
MOHAMED SLIM, HANADI SLEIMAN,
- 205 ANALYSIS OF SOME NATURAL SUBSTANCES BY CPG USING A BINARY MIXTURE OF LIQUID CRYSTALS AS STATIONARY PHASE  
S. SEBIH, F. ATHMAN, S. BOUDAH
- 207 CHARACTERIZATION OF ALLOY STEELS PRODUCED BY SINTERING Fe<sub>0.4</sub>C<sub>0.2</sub>CU<sub>0.2</sub>NIO<sub>0.7</sub>MO AND Fe<sub>1.4</sub>C<sub>0.2</sub>CU<sub>0.2</sub>NIO<sub>0.7</sub>MO  
SAID MÈCHACHTI, SALIM SERRAI, OMAR BENCHIEUB
- 215 DETERMINATION OF METHYL MERCURY AND INORGANIC MERCURY IN NATURAL WATERS USING ETHYLATION OR PROPYLATION COMBINED WITH AN AUTOMATED PURGE AND TRAP - GAS CHROMATOGRAPHY - PYROLYSIS - ATOMIC FLUORESCENCE SPECTROMETRY SYSTEM (MERX-M)  
ABUBAKER SHARIF
- 219 DETERMINATION OF POLYCHLORINATED BIPHENYLS (PCBS) IN CONTAMINATED SOILS  
A. TOUABET, A. HALFADJI
- 221 ELECTROLUMINESCENT PROPERTIES OF LIGHT-EMITTING ELECTROCHEMICAL CELLS BASED ON CATIONIC IRIIDIUM COMPLEXES WITH OXAZOLE-BASED ANCILLARY LIGANDS  
JIYOUNG HEO AND YOUNGSON CHOE
- 223 LIQUID CRYSTALS STATIONARY PHASES USE FOR THE ANALYSIS OF VOLATILE AROMA COMPOUNDS IN ESSENTIAL OILS  
S. BOUDAH, S. SEBIH, J.P. BAYLE
- 225 NANOSTRUCTURED ACID/BASE MATERIALS VIA NITRIDATION  
ABDELRAHMAN ALI AND ROBERT MOKAYA
- 237 SEPARATION OF STAPHYLOCOCCUS AUREUS CAUSING SERIOUS INFECTIONS BY ELECTROPHORETIC TECHNIQUES  
MARIE VYKDALOVA-TESAROVA, MARIE HORKA, DANA MORAVCOVA, LENKA STAVIKOVA, FILIP ROZICKA
- 239 SORPTION BEHAVIOUR OF LEAD, CADMIUM, COPPER, AND ZINC IN MINE SOIL  
LOTFI MOUINI, LAZHAR BELKHRI, ABDELKRIM BOUZAZA, FATEH ZOUGGAGHE, MOURAD TAFRE
- 245 STUDY OF THE RESISTANCE TO CRACK PROPAGATION IN THERMAL INSULATION MATERIALS  
SEDDIK BOURAS, INES ZERZER AND FARID GHELDANE
- 247 SURFACE PARAMETERS AND THERMO-GRAVIMETRIC ANALYSIS FOR PARENT AND MODIFIED NANO-ZEOLITES CORRELATED WITH THEIR CATALYTIC ACTIVITY  
SAMAA M. SOLYMAN
- 261 SYNTHESIS OF APPROPRIATE OLEAGINOUS BIOMASS FOR BIOFUEL PRODUCTION  
A. C. AHMIA, F. DANANE, R. BESSAH, R. ALLOUNE, M. AZIZA
- 267 EFFECT OF COBALT AND ANTIMONY ON ZINC ELECTROWINNING USING SULFATE SOLUTIONS  
VLADISLAVA STEFANOVA, ERDUAN MEHMED, PETAR ILEY, BISERKA LUCHEVA
- 279 STRUCTURAL, MORPHOLOGICAL AND SWELLING PROPERTIES OF NOVEL POLY(NMAA-CO-HEA)/MG-AL-CL LAYERED DOUBLE HYDROXIDE NANOCOMPOSITE HYDROGELS  
ÖZLEM YILMAZ, AYÇA BAL, MEHMET KORAY GÖK, GAMZE GÜÇLÜ, SAADET PABUCCUOĞLU
- 289 SYNERGISTIC EFFECT OF YTTRIUM NITRATE AND POTASSIUM IODIDE ON THE INHIBITION OF THE CORROSION OF CARBON STEEL A37 IN H2SO4 0,5M  
SHEM OUCHEHANE, SHEM ABDERRAHMANE, AMEL SEDIK, SAMEH ATHMANI
- 301 THERMODYNAMIC STUDY OF THE CYSTEINE ADSORPTION ON COPPER SURFACE IN HNO3 1M  
AMEL SEDIK, SHEM ABDERRAHMANE, SHEM OUCHEHANE, AMEL GHARBI
- 303 CHARACTERIZATION STUDY OF SEPIOLITE AND BOROGLYPSUM MINERALS FOR THE SYNTHESIS OF NEW GENERATION MATERIALS  
F. T. SENBERBER AND S. PISKIN
- 311 CFD SIMULATIONS FOR BENZENE NITRATION REACTION IN A MICROREACTOR  
S. KOUADRI MOUSTEFAI, W. HARCHOUICHE, B. BENSABER
- 313 ELIMINATION OF HERBICIDE THE METRIBUZIN (C8H14N4O5) BY THE METHOD OF ADSORPTION ON DIFFERENT MEDIA ADSORBENTS TO KNOW: THE MAGHINITE MAGHINIA THE CHARCOAL (POWDER - GRAIN) AND THE ZEOLITES  
B. A. REGUIG, A. BETTAÏEB, A. YAHIAOUI, A. BENYUCEF
- 315 INDEX

## STRUCTURAL, MORPHOLOGICAL AND SWELLING PROPERTIES OF NOVEL POLY(NAAA-CO-HEA)/ MG-AL-CL LAYERED DOUBLE HYDROXIDE NANOCOMPOSITE HYDROGELS

Özlem Yılmaz, Ayça Bal, Mehmet Koray Gök, Gamze Güçlü, Saadet Pabuccuoğlu  
Istanbul University, Faculty of Engineering, Chemical Engineering Department, Avcılar-  
Istanbul, 34320, Turkey.  
aycabal@gmail.com

### Abstract

The objective of this study is to investigate the effects of the Mg-Al-Cl layered double hydroxide (Mg-Al-Cl LDH) on the swelling, morphological and structural properties of the poly(sodium acrylate-co-2-hydroxyethyl acrylate) [poly(NAAA-co-HEA)] hydrogel. Acrylate monomer based novel nanocomposite hydrogels containing Mg-Al-Cl LDH [poly(NAAA-co-HEA)/ Mg-Al-Cl LDHs] were synthesized by using the equal mole amounts of NaAA and HEA as monomers, potassium persulfate-bisulfite as initiator, N,N-methylenebisacrylamide (NMBA) as cross-linker and different amounts (1, 3, 5 % of total monomer weight) of Mg-Al-Cl LDH. The formation, morphological and structural properties of poly(NAAA-co-HEA)/Mg-Al-Cl LDHs were investigated by Fourier Transform Infrared (FTIR) Spectroscopy, X-ray Diffraction (XRD) Pattern and Scanning Electron Microscopy (SEM) analyses. Swelling behaviors of poly(NAAA-co-HEA)/ Mg-Al-Cl LDHs were also examined in distilled water. The results show that poly(NAAA-co-HEA)/ Mg-Al-Cl LDHs have been formed. As the content of Mg-Al-Cl LDHs increased, equilibrium swelling degree of the nanocomposite hydrogels in distilled water decreased due to the Mg-Al-Cl LDHs acting as crosslinking agent. It is then concluded that the poly(NAAA-co-HEA)/ Mg-Al-Cl LDHs synthesized in this study may be used as an alternative water absorbent.

**Keywords:** Mg-Al-Cl Layered double hydroxides, nanocomposite hydrogels, 2-hydroxyethyl acrylate, sodium acrylate.

### Introduction

The layered double hydroxides (LDHs), also called anionic clays, are composed of positively charged layers with interlayer exchangeable anions. LDHs have physical and chemical properties that are surprisingly similar to the properties of clay mineral. Its general composition can be represented as  $[M^{II}_{1-x}M^{III}_x(OH)_2]^{+x} [A^{n-}]_{x/n} \cdot nH_2O$ , where  $M^{II}$  and  $M^{III}$  are divalent and trivalent cations, respectively, and  $A^{n-}$  is an exchangeable anion (Lee et al., 2005). The layer metal cations can be chosen among a wide selection, such as  $Mg^{2+}$ ,  $Ni^{2+}$ ,  $Zn^{2+}$ ,  $Al^{3+}$ ,  $Fe^{3+}$ , etc., as with the interlayer anion (Figure1), that can be inorganic or organic in nature (Ardanuy et al., 2010). In recent years, LDHs have been used as nanoparticles for preparing

polymer-based nanocomposites. The use of LDHs as nanoparticles is advantageous due to their versatility in chemical composition and allow multiple interactions with the polymer (Özgümüş et al., 2013; Kovanda et al., 2010; Hoyo et al., 2007).

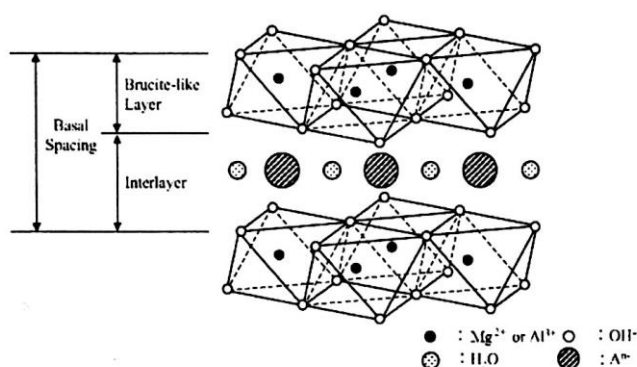


Figure 1. Schematic representation of Mg-Al LDH (Ardanuy et al., 2010).

In this study, the effects of the Mg-Al-CI layered double hydroxide (Mg-Al-CI LDH) on the swelling, morphological and structural properties of the poly(NaAA-co-HEA) hydrogel were investigated. In our previous study, Mg-Al-CI LDH was prepared by the coprecipitation method and characterized using FTIR, XRD and SEM techniques (Özgümüş et al., 2013). Acrylate monomer based novel nanocomposite hydrogels containing Mg-Al-CI LDH [poly(NaAA-co-HEA)/ Mg-Al-CI LDHs] were synthesized by using NaAA and HEA as monomers, potassium persulfate-bisulfite as initiator, NMBA as cross-linker and different amounts (1, 3, 5 % of total monomer weight) of Mg-Al-CI LDH. The formation, morphological and structural properties of poly(NaAA-co-HEA)/ Mg-Al-CI LDHs were investigated by FTIR, XRD and SEM analyses. Swelling behaviors of poly(NaAA-co-HEA)/ Mg-Al-CI LDHs were also examined in distilled water.

**Experimental**

**Preparation of Nanocomposite Hydrogels**

Novel poly(NaAA-co-HEA)/ Mg-Al-CI LDHs (NH-LDHs) containing Mg-Al-CI LDH, synthesized in our previous study (Özgümüş et al., 2013), were prepared by free radical chain polymerization of NaAA and HEA in Mg-Al-CI LDH suspension. Firstly, Mg-Al-CI LDH was suspended in water thoroughly under ultrasonic irradiation. NaAA and HEA monomers and NMBA (0.5% of total monomer moles) were dissolved in suspended Mg-Al-CI LDH and taken in cylindrical glass tubes. After sealing the tubes with rubber caps, the solution was purged with nitrogen gas for 20 min eliminate dissolved oxygen in the system. The polymerization was performed at 80°C by introducing of initiator (1 X 10<sup>-4</sup> mole) (1% of total monomer moles). After 3h reaction time at 80°C, the hydrogels were separated, cut into discs in 5-mm length and washed with water for 1 week. Then, nanocomposite hydrogels

were dried and prepared with conditions appli

Symbols hydrog

H

NH-1L

NH-3L

NH-5L

Table

Swelling St

The swellin distilled water The amount o swelling degre

$$Q_e = (W_{wet} -$$

where W<sub>sw</sub> swollen sampl

Instrumen

FTIR spectri using Digilab I the range of 4 XRD patte Diffractomete scanning spee The scanni using a Quan microscopy.

Results an

XRD Anal

Figure 2 ill Al-CI LDH and % Mg-Al-CI LDH

advantageous reactions with (2007).

○ : OH-  
● : A<sup>-</sup>

(2010).

ide (Mg–Al–Cl poly(NaAA–Cl LDH was XRD and SEM nanocomposite [LDHs] were sulfate–bisulfite total monomer al properties XRD and SEM ts were also

ng Mg–Al–Cl prepared by suspension. er ultrasonic omer moles) l glass tubes. with nitrogen erization was tal monomer cut into discs site hydrogels

were dried under vacuum at 40°C. The hydrogel poly(NaAA-co-HEA) (H) was also prepared without using Mg–Al–Cl LDH to compare the results. Details about the conditions applied to synthesize the nanocomposite hydrogels are listed in Table 1.

Symbols of the hydrogels	Monomers NaAA/HEA (mole)	NMBA (mole %)	Mg–Al–Cl LDH (wt %)
H	0.005/0.005	5x10 <sup>-5</sup>	0
NH-1LDH	0.005/0.005	5x10 <sup>-5</sup>	1
NH-3LDH	0.005/0.005	5x10 <sup>-5</sup>	3
NH-5LDH	0.005/0.005	5x10 <sup>-5</sup>	5

Table 1. The feed compositions of the nanocomposite hydrogels.

#### Swelling Studies of the Nanocomposite Hydrogels

The swelling characteristics of the nanocomposite hydrogels were measured in distilled water through, tea-bag method, gravimetric analysis (Dalaran et al., 2009). The amount of the water absorbed by the samples was given as the equilibrium swelling degree ( $Q_{eq}$ ) and was calculated by eq. (1).

$$Q_e = (W_{wet} - W_{dry}) / W_{dry} \quad (1)$$

where  $W_{dry}$  is the weight of the dried sample and  $W_{wet}$  is the weight of the swollen sample.

#### Instruments

FTIR spectra of the samples were taken as KBr disks (sample/ KBr=1/250, w/w) using Digilab Excalibur-FTS 3000MX model FTIR Spectrophotometer operating in the range of 4000–650 cm<sup>-1</sup>.

XRD patterns were obtained using a Rigaku D/Max-2200/PC X-Ray Powder Diffractometer (Japan) using CuK $\alpha$  radiation ( $\lambda=1.5406$  nm) at 30 mA, 40 kV, a scanning speed of 1°/min from 2 $\theta=5^\circ$  to 2 $\theta=30^\circ$ .

The scanning electron microscopy (SEM) images of the samples were obtained using a Quanta FEG 450 Scanning Electron Microscopy (USA) scanning electron microscopy.

#### Results and Discussion

##### XRD Analysis

Figure 2 illustrates the typical diffraction peak from XRD powder patterns of Mg–Al–Cl LDH and the corresponding nanocomposite hydrogel incorporated with 3 wt. % Mg–Al–Cl LDH (NH-3LDH).

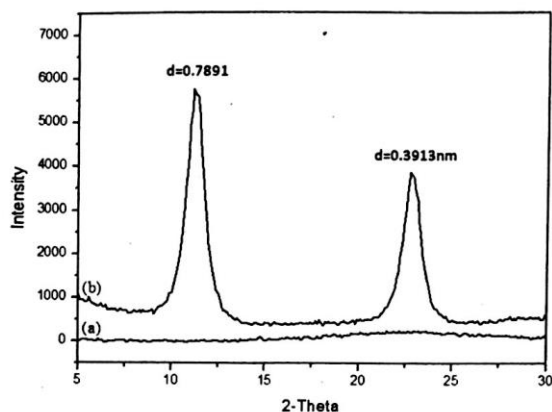


Figure 2. XRD patterns of (a) NH-3LDH (b) Mg-Al-CI LDH.

There are two intense diffraction peaks for Mg-Al-CI LDH, the main strong peak approximately at  $2\theta = 11.3^\circ$  corresponding to  $d = 0.7891$  nm and the other sharp peak approximately at  $2\theta = 22.9^\circ$  corresponding to  $d = 0.3913$  nm, while no diffraction peak appears for nanocomposite hydrogel sample NH-3LDH (3 wt% Mg-Al-CI LDH), it was attributed that Mg-Al-CI LDH sheets are exfoliated and uniformly dispersed in poly(NaAA-co-HEA) hydrogel network.

#### FT-IR Analysis

FTIR analysis reveals that the nature of change in hydrogel matrix and Mg-Al-CI LDH during the formation of the nanocomposite. The FTIR spectra of Mg-Al-CI LDH, H and NH-3LDH are shown in Figure 3a. FTIR spectrum of the Mg-Al-CI LDH showed characteristic absorption bands; the intense and broad band at about  $3200\text{--}3700$   $\text{cm}^{-1}$  region (max. at  $3510$   $\text{cm}^{-1}$ ) was related to the asymmetric and symmetric stretching mode of hydrogen-bonded OH groups in the hydroxyl layers; the small shoulder at approximately  $3050$   $\text{cm}^{-1}$  was assigned to hydroxyl interactions with carbonate ions impurities in the interlayer, and has been attributed to the bridging mode  $\text{H}_2\text{O}\text{--}\text{CO}_3^{2-}$ . The weak absorption band corresponding to the  $\text{H}_2\text{O}$  deformation bending vibration was also seen at  $1653$   $\text{cm}^{-1}$  as a function of the interlamellar anions such as  $\text{CO}_3^{2-}$ . The sharp absorption band at  $1372$   $\text{cm}^{-1}$ , the small shoulder and weak band at  $863$  and  $651$   $\text{cm}^{-1}$  attributed to unidentate carbonate symmetric stretching vibrations (O-C-O bond) for the LDH with  $\text{CO}_3^{2-}$  anions incorporated into the interlayer. An additional broad shoulder at  $1500\text{--}1550$   $\text{cm}^{-1}$  regions attributed to the formation of bicarbonate ions due to the proton transfer from the hydroxide sheets to the carbonate ion. A series of bands in spectra which were recorded at  $1000\text{--}400$   $\text{cm}^{-1}$  region are complicated due to the presence of lattice translational modes (Özgümüş et al., 2013).

In the spectra of the H Figure 3c the characteristic band at  $3449$   $\text{cm}^{-1}$ ,  $2957$  and  $1579$   $\text{cm}^{-1}$  was attributed to the the asymmetric and symmetric stretching mode

of OH groups in the HEA units on the copolymer structure, stretching vibration of  $\text{CH}_2$  groups and C=O asymmetric stretching in the carboxylate anion, respectively. This was confirmed by another peak at  $1405\text{--}1400\text{ cm}^{-1}$  region (max.  $1415\text{ cm}^{-1}$ ), which is related to the symmetric stretching mode of the carboxylate groups and OH groups of the HEA monomer units. The main contribution to the absorption band at  $1732\text{ cm}^{-1}$  is from the C=O bonds stretching vibrations of the ester groups of HEA monomer units. Other bands at

$1167$ ,  $1078$  and  $888\text{ cm}^{-1}$  corresponding to the C-O bonds vibrations of the monomers units, and OH groups vibrations of the monomer units were observed, respectively (Sadeghi et al., 2013).

The overall changes in the structure of Mg-Al-CI LDH and H, depending on the formation of the NH-3LDH with exfoliated structure, were also investigated by FTIR analysis. A careful comparison of all the FTIR spectra indicates definite differences mainly in the absorption bands, appearing at approximately at  $1750\text{--}1500\text{ cm}^{-1}$ ,  $1500\text{--}1300\text{ cm}^{-1}$  and  $1000\text{--}600\text{ cm}^{-1}$ . As observed from the NH-3LDH spectra, the absorption bands observed at  $3050$ ,  $1653$ ,  $1372$  and  $1000\text{--}600\text{ cm}^{-1}$  (max at  $863$ ,  $750$  and  $651\text{ cm}^{-1}$ ) in the FTIR spectra of the Mg-Al-CI LDH disappeared. All these changes and the disappearances of some bands are associated with the formation of the NH-3LDH with exfoliated structure. Namely, the monomers NaAA and HEA, the crosslinker NMBA and Mg-Al-CI LDH physically or chemically interacted to form a network structure during the copolymerization reaction. Therefore, the layers of the Mg-Al-CI LDH were exfoliated. These results are consistent with those of the powder XRD spectra for Mg-Al-CI LDH, H and NH-3LDH.

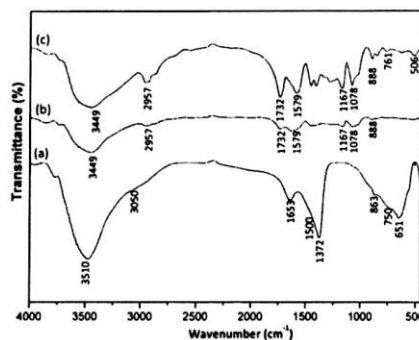


Figure 3. FTIR spectra of (a) Mg-Al-CI LDH (b) NH-3LDH nanocomposite hydrogel and (c) H hydrogel.

#### SEM Analysis

In order to examine the surface morphology of the Mg-Al-CI LDH, H and NH-3LDH, the SEM micrograph were taken at different magnification. Figure 4-6 represent the SEM micrographs for these products. Micrograph, is shown in Figure 4, revealed that Mg-Al-CI LDH exhibits bead-like fine particle aggregates consisting of nanometer size (Özgümüş et al., 2013). The SEM images of H hydrogel (Figure



5) also demonstrate that H hydrogel has porous surface. NH-3LDH nanocomposite hydrogel showed some interesting morphological features when compared to H hydrogel (Figure 6). In addition, it can be seen from SEM images that the NH-3LDH nanocomposite hydrogel has a fiber-like structure, non-porous surface morphology and also exhibited large, open, channel-like structure, its shape is significantly different than that of the Mg-Al-Cl LDH and H. These results are also increasing evidence the occurrence of fully exfoliation between the Mg-Al-Cl LDH layers and H during the formation of the NH-3LDH nanocomposite hydrogel, as demonstrated our earlier study (Özgümüş et al., 2013).

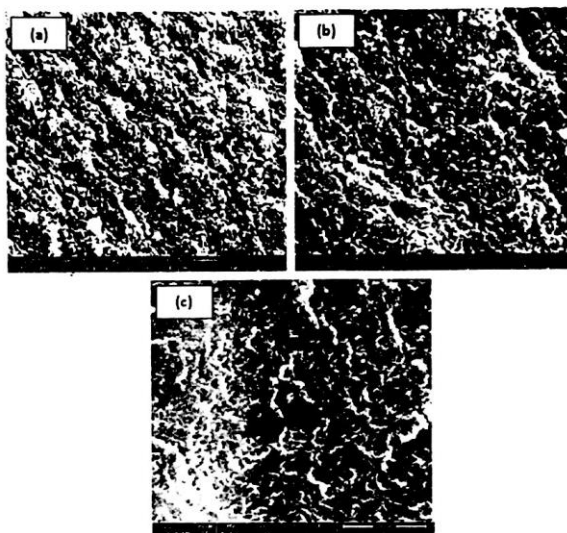


Figure 4. SEM images of Mg-Al-Cl LDH at different magnification: (a)40000x, (b) 80000x and (c) 150000x.

nanocomposite compared to H at the NH-3LDH ice morphology is significantly also increasing LDH layers and s demonstrated

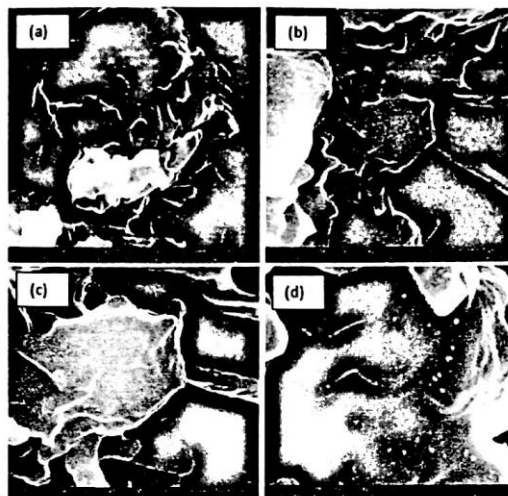


Figure 5. SEM images of H hydrogel at different magnification: (a)40000x, (b) 80000x, (c) 150000x and (d) 300000x.

(a)40000x, (b)

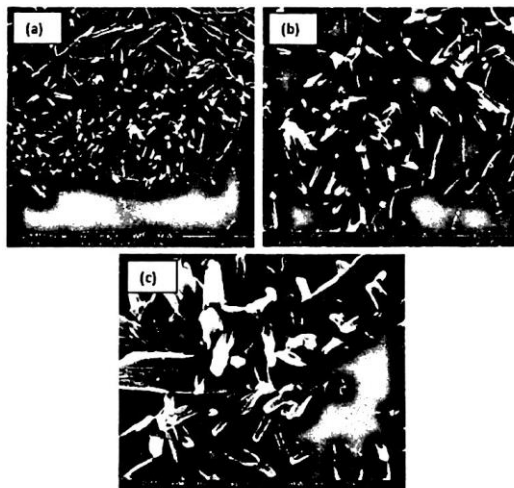
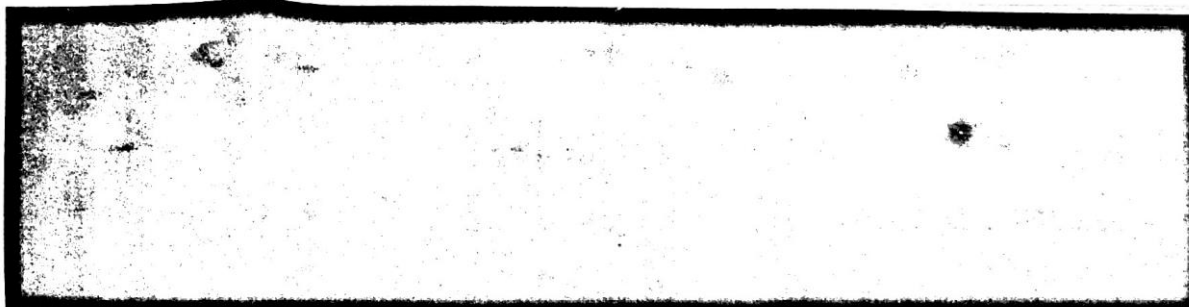


Figure 6. SEM images of NH-3LDH at different magnification: (a)40000x, (b) 80000x and (c) 150000x.



#### Effect of Mg–Al–Cl LDH Content on Swelling Capacity

The data in Figure 7 clearly showed also that, swelling capacity of the nanocomposite hydrogels decreased 30%, 48% and 82% with increasing amount of Mg–Al–Cl LDH from 1 to 5 wt%, respectively. Mg–Al–Cl LDH, which are called hydrotalcite-like compound, it is incorporated into the polymer matrix, may acts as additional co-crosslinking points similar to clay powder. The reason for the decrease in the  $Q_e$  value of the NH-LDHs is most likely due to the additional co-crosslinking points effect of the Mg–Al–Cl LDH (Özgümüş et al., 2013).

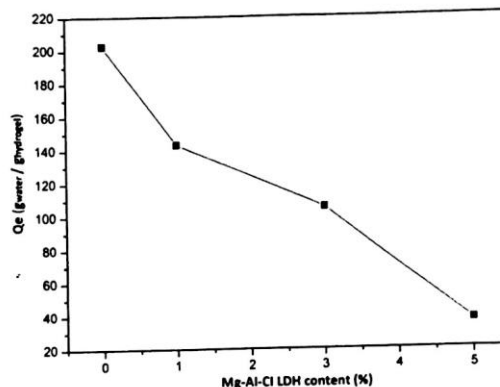


Figure 7. The effect of the content of Mg–Al–Cl LDH on the water absorbency of nanocomposite hydrogels

#### Conclusion

A series of nanocomposite hydrogels containing Mg–Al–Cl LDH [poly(NaAA-co-HEA)/ Mg-Al-Cl LDHs] were synthesized by free radical chain polymerization of NaAA and HEA in Mg–Al–Cl LDH suspension. FTIR analysis showed that the nanocomposite hydrogels were successfully obtained. Furthermore, XRD analysis of the samples showed that Mg–Al–Cl LDH layers were exfoliated in the hydrogel structure. According to the SEM images, NH-3LDH has a fiber-like structure, non-porous surface morphology and its shape is significantly different from that of the Mg–Al–Cl LDH and H. Swelling studies showed that swelling capacity of the nanocomposite hydrogels decreased 30%, 48% and 82% with increasing amount of Mg–Al–Cl LDH from 1 to 5 wt%, respectively. It is then concluded that the poly(NaAA-co-HEA)/ Mg-Al-Cl LDHs synthesized in this study may be used as an alternative water absorbent.

**Acknowledgments** The present work was supported by the Research Fund of Istanbul University; Project Numbers 6940 and 15841.

capacity of the  
easing amount  
which are called  
rix, may acts as  
or the decrease  
co-crosslinking

absorbency of

PH [poly(NaAA-  
polymerization  
owed that the  
e, XRD analysis  
in the hydrogel  
-like structure,  
erent from that  
capacity of the  
easing amount  
luded that the  
be used as an

search Fund of

#### References

- Ardanuy, M., Velasco, J.I., Antunes, M., Rodriguez Perez, M.A., Saja, J.A., 2010, Structure and properties of polypropylene/hydrotalcite nanocomposites, *Polym. Compos.*, 31(5) 870–878.
- Dalaran, M., Emik, S., Güçlü, G., İyim, T.B., Özgümüş, S., 2009, Removal of acidic dye from aqueous solutions using poly(DMAEMA–AMPS–HEMA) terpolymer/MMT nanocomposite hydrogels, *Polym. Bull.*, 63, 159–171.
- Hoyo, C.D., 2007, Layered double hydroxides and human health: an overview, *Appl. Clay Sci.*, 36, 103–121.
- Kovanda, F., Jindova, E., Lang, K., Kubat, P., Sedlakova, Z., 2010, Preparation of layered double hydroxides intercalated with organic anions and their application in LDH/poly(butyl methacrylate) nanocomposites, *Appl. Clay Sci.*, 48, 260–270.
- Lee, W.F., Chen, Y.C., 2005, Effect of Intercalated Hydrotalcite on Swelling and Mechanical Behavior for Poly(acrylic acid-co-N-isopropylacrylamide)/Hydrotalcite Nanocomposite Hydrogels, *Journal of Applied Polymer Science*, 98, 1572–1580.
- Özgümüş, S., Gök, M.K., Bal A., Güçlü, G., 2013, Study on novel exfoliated polyampholyte nanocomposite hydrogels based on acrylic monomers and Mg–Al–Cl layered double hydroxide: Synthesis and characterization, *Chemical Engineering Journal*, 223, 277–286.
- Sadeghi, M., Hosseinzadeh, H., 2013, Synthesis and properties of collagen-g-poly(sodium acrylate-co-2-hydroxyethylacrylate) superabsorbent hydrogels, *Brazilian Journal of Chemical Engineering*, 30(2), 379–389.